RMetS

Royal Meteorological Society

Interannual and interdecadal variations of tropical cyclone activity in the South China Sea

Andy Zung-Ching Goh and Johnny C. L. Chan*
Guy Carpenter Asia-Pacific Climate Impact Centre, City University of Hong Kong, Hong Kong, China

ABSTRACT: This study attempts to identify the factors affecting annual tropical cyclone (TC) activity in the South China Sea (SCS) using data during the period 1965–2005. The results indicate that the total number of TCs and number of TCs entering the SCS from the Western North Pacific are below normal in El Niño events but above normal during La Niña events. However, for TCs formed inside the SCS, the difference in numbers between the two phases of the El Niño-Southern Oscillation (ENSO) is not as obvious. In addition, the positive phase of the Pacific Decadal Oscillation (PDO) generally favours less TCs in all categories, while the negative PDO phase favours more. These results may be explained by the fact that the ENSO and the PDO affect TC behaviour through altering the conditions in the WNP to be favourable or unfavourable for TC genesis and movement into the SCS. Copyright © 2009 Royal Meteorological Society

1. Introduction

Tropical cyclones (TCs) are one of the deadliest and costliest natural disasters, especially for those who live near coastal areas. As a huge population lives along the coast of southern China, it is of significant interest to understand and accurately predict TC behaviour in the South China Sea (SCS). However, this has been a relatively less studied area.

Owing to their proximity, the behaviour of TCs in the western North Pacific (WNP) could shed some light on those in the SCS. Previous research has shown that TC activity in the WNP exhibit variations on interannual (e.g. Chan, 1985), interdecadal (e.g. Chan and Shi, 1996) and long-term (e.g. Yeung *et al.*, 2005) time scales. Such variations have been related to the El Niño-Southern Oscillation (ENSO) (e.g. Chan, 1985, 2000; Chen *et al.*, 1998; Wang and Chan, 2002), Pacific Decadal Oscillation (PDO) (Leung *et al.*, 2005), and Quasi-Biennial Oscillation (QBO) in the stratosphere (Chan, 1995). As ENSO has a well-documented effect on TC activity, and PDO has also been shown to be possibly forced by ENSO (e.g. Newman *et al.*, 2003; Yeh and Kirtman, 2004; Schneider and Cornuelle, 2005), the focus of this study is on the ENSO and the PDO and their respective effects on TC activity in the WNP, while the effect of the QBO is not included.

Gray (1968, 1979) identified six factors, three dynamic and three thermodynamic, for TC genesis and development, namely, the Coriolis parameter, low-level (850-hPa) vorticity, vertical shear of the horizontal wind, mid-level moisture, moist instability of low- to mid- (500-hPa) troposphere, and sea surface temperature (SST). These factors are therefore discussed in this paper.

The vorticity related to the monsoon trough at 850 hPa (Chia and Ropelewski, 2002; Wang *et al.*, 2007b) and the strong outflow due to divergence at 200 hPa (Yumoto and Matsuura, 2001) are apparently important to TC formation, which have also been discussed by Briegel and Frank (1997). In addition, Liu and Chan (2006) stressed the effect of the 850-hPa geopotential height on TC genesis and McBride and Zehr (1981) indicated that vertical shear should be at a minimum at, but large around, the centre where TCs form.

Many studies have indicated that a high SST is favourable for TC formation and intensification (e.g. Gray, 1979; Ho *et al.*, 2004), although some suggested that local SST is not of major concern (e.g. Lighthill *et al.*, 1994; Chan and Liu, 2004; Ramsay *et al.*, 2008). Stowasser *et al.* (2007) discussed the effect of global warming on the formation of TCs, which could present some problems when using moist static energy (MSE), suggested by Chan and Liu (2004), as a genesis factor. However, as Emanuel (1993) pointed out, the moisture in the lower troposphere is also important in determining TC formation, so MSE should still be included as a possible factor.

Movement of TCs is affected by both external (Neumann, 1992) and internal (Chan and Williams, 1987, 1994) factors. George and Gray (1976) and Chan and

* Correspondence to: Johnny C. L. Chan, Guy Carpenter Asia-Pacific Climate Impact Centre, City University of Hong Kong, Tat Chee Avenue, Kowloon, Hong Kong, China.
E-mail: johnny.chan@cityu.edu.hk

Gray (1982) related the 500-hPa flow to the steering of TCs, while Ho *et al.* (2004) and Lee *et al.* (2006) both suggested the subtropical high as a steering factor.

It has long been known that ENSO plays a role in shaping the climate in East Asia. It not only affects the formation location and subsequent motions of TCs in the WNP (e.g. Chan, 2000; Wang and Chan, 2002; Chan, 2005) and the SCS (Liu and Chan, 2003) but also the number of TCs in both basins (Li, 1988) and the number of landfalls in southern China (Wu *et al.*, 2004). On the other hand, Liu and Chan (2003) found that TC movement is affected by ENSO, and Leung *et al.* (2005) further suggested that TC activity in the SCS is modulated by PDO. As some studies (e.g. Hare and Mantua, 2000) have pointed out the climatic and biological impacts of the PDO phase shifted around 1976, it is possible that this phenomenon is also a factor affecting TC behaviour.

The objective of this study is therefore to investigate the effects of ENSO and PDO on TC behaviour in the SCS. Section 2 of this paper introduces the data used in this study. This is followed by a study of the interannual and interdecadal variations in TC activity in Section 3. The reasons for these variations and the factors responsible are investigated in Section 4. A final discussion and conclusion can be found in Section 5.

2. Data

2.1. Data

TC data from the Hong Kong Observatory and atmospheric data from the National Centers for Environmental Prediction–National Center for Atmospheric Research (NCEP–NCAR) Reanalysis Project (Kalnay *et al.*, 1996) are used. As data before 1965 are likely to have large uncertainties (e.g. Song *et al.*, 2002; Wu *et al.*, 2005), only TCs after 1965 are utilized in this study. ENSO data are from the Climate Prediction Center of the US National Weather Service (http://www.cpc.ncep.noaa.gov/products/analysis_monitoring/ensostuff/ensoyears.shtml), while PDO data are from the University of Washington's Joint Institute for the Study of the Atmosphere and Ocean (http://jisao.washington.edu/pdo/PDO.latest).

2.2. Data categorization

For this study, only TCs that had attained at least tropical storm strength (maximum wind speed >65 km h^{-1}) are included. The SCS is defined to be the ocean body within 0°N and 25°N, and 100°E and 120°E. The WNP extends to 180°. TCs in the SCS are first divided into those that are formed within the SCS (FORM) and those that entered the SCS from the WNP (ENT) according to the following criteria:

1. Any TC that formed within the defined SCS boundary, including those formed on the boundary itself, would be considered as FORM, and any TC formed outside

of the SCS, but had at least one recorded 6-hourly position within the SCS would be considered as ENT, regardless of whether it would eventually move out of the area.
2. ENT would not include those that formed in the SCS to start with.
3. TCs that entered the SCS, then moved out, and subsequently entered again would only be counted once.

Previous studies have suggested that the active TC season in the SCS is between May and November (Liu and Chan, 2003; Wang *et al.*, 2007a), and that this period can be divided into an "early" and a "late" season (Liu and Chan, 2003). It is therefore useful to divide the TC season in the SCS into May to August (early season) and September to December (late season). This division is such that each season has the same number of months, and the number of FORM (N_F) and number of ENT (N_E) in each season are about the same (86 in early *vs* 68 in late for N_F, and 105 *vs* 138 for N_E).

Trenberth (1997) defined an ENSO index using a threshold of ±0.4 °C. The period in which the index is above +0.4 °C is defined an EN event and an LN event if this index is below −0.4 °C. An EN or an LN year is the onset year of the respective event. According to this, 12 EN events and 10 LN events are found in the 41 years from 1965 to 2005. Following Mantua (1999), the winter/spring (October–March) average value of the PDO indices is used in this study to determine the phase of the PDO. A year is designated as PDO positive or negative according to whether the index is greater or less than its mean value by half a standard deviation, namely, 0.42 and −0.50, respectively. In total, there were 16 PDO+ and 13 PDO− events between 1965 and 2005.

3. Interannual and interdecadal variations in TC activity

3.1. Trend analysis

Interannual and interdecadal variabilities of TC activity in the WNP are apparent in the SCS. The average total number of TCs (N_T), N_E, and N_F in the whole season for the period of 1965–2005 is 9.8, 6.0, and 3.8, respectively. The whole season also sees a decreasing trend in N_T, N_E, and N_F of −5.7, −5.2, and −0.2 per 100 years over the study period (Figure 1(a), (b) and (c)), with those in N_T and N_E being significant at the 95% confidence level. The significance in the trend is determined using the method in Santer *et al.* (2000).

In the early season, the average N_T, N_E, and N_F are 4.7, 2.6, and 2.1, respectively. The N_F series shows an insignificant trend, with an increase of 0.2 per 100 years between 1965 and 2005 (Figure 2(c)). On the other hand, the trends in both the N_T and N_E series are significant at the 95% level, with a rate of −2.4 and −2.6 per 100 years over the same period (Figure 2(a) and (b)). For the late season, the average N_T, N_E, and N_F are 5.1, 3.4, and
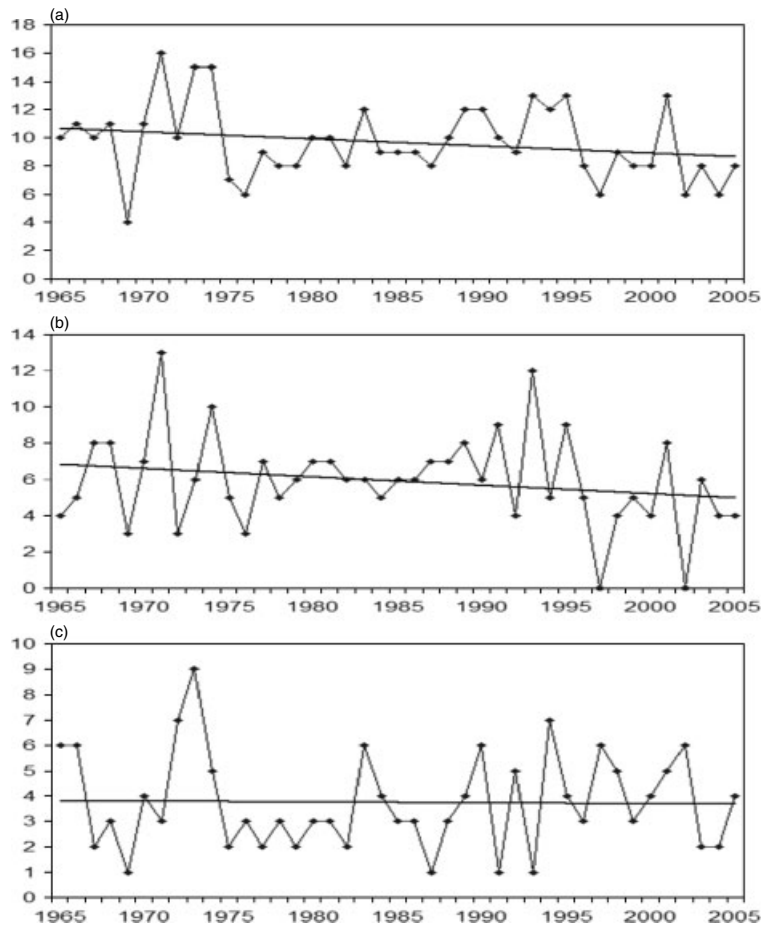
Figure 1. (a) Total number of TCs (N_T), (b) number of TCs entering (N_E) and (c) number of TCs formed (N_F) in the SCS during the whole season. The solid straight line indicates the trend.

1.7, respectively. Again, only N_T, N_E show statistically significant decreasing trends over the study period, the rates being -2.6, -2.1 per 100 years (Figure 3(a) and (b)), while the trend for N_F is not statistically significant at -0.5 per 100 years (Figure 3(c)).

3.2. Periodicity of TC occurrences

A wavelet analysis with the Mexican-hat wavelet (Derivative of Gaussian with $m = 2$) as the basis function is employed to estimate the periodicity of TC occurrences in the basin. This basis function gives a much finer scale structure, because it is real-valued and could capture both the positive and negative oscillations of the time series as separate peaks in wavelet power (Torrence and Compo, 1998).

Before, around 1976 or 1977, N_E in the whole season (Figure 4(a)) exhibits a 2- to 6-year periodicity, while that of N_F (Figure 4(b)) has a periodicity of 5–8 years. After that, the period of 2–6 years could again be seen between 1990 and 2003 for N_E, while no clear periodicity could be seen in N_F. Separately, in the early season, N_E shows a period of 8–16 years (Figure 4(c)) that extends over the whole data range. A periodicity of 4–8 years is found in the FORM series (Figure 4(d)) before 1975. After that, a periodicity of 2–8 years is found in N_F between 1990 and 2003. On the other hand, in the late season, there is a 2-

to 6-year period in N_E before 1977 (Figure 4(e)), and the period shifts to more than 16 years after that. Similarly, there is a periodicity of 8–20 years in N_F (Figure 4(f)) before 1980, which decreases to 4–8 years in the 1980s. After that, no periodicity can be seen until between 1995 and 2000 when a period of 2–8 years is found.

It is apparent from these results that TC activity in the SCS has a decreasing trend and possesses significant interannual and interdecadal variabilities, with periods ranging from 2 to over 10 years. The shorter periodicity coincides with the period of ENSO, which is around 3–7 years, suggesting that ENSO may be related to the number of TCs in the SCS. However, as there are only 41 years of data, longer periods cannot be identified. Nonetheless, the periodicities that are over 16 years might be related to the PDO, as its period can range from 20 to 30 years.

3.3. TC behaviour during different phases of the ENSO and the PDO

In general, fewer N_T, N_E, and N_F are found during EN in the late and whole seasons, but no obvious difference exists in the early season (Table I). In the late season, the differences between EN and LN in all three categories are significant at the 95% confidence level, but none of the differences in the early season is. A similar situation
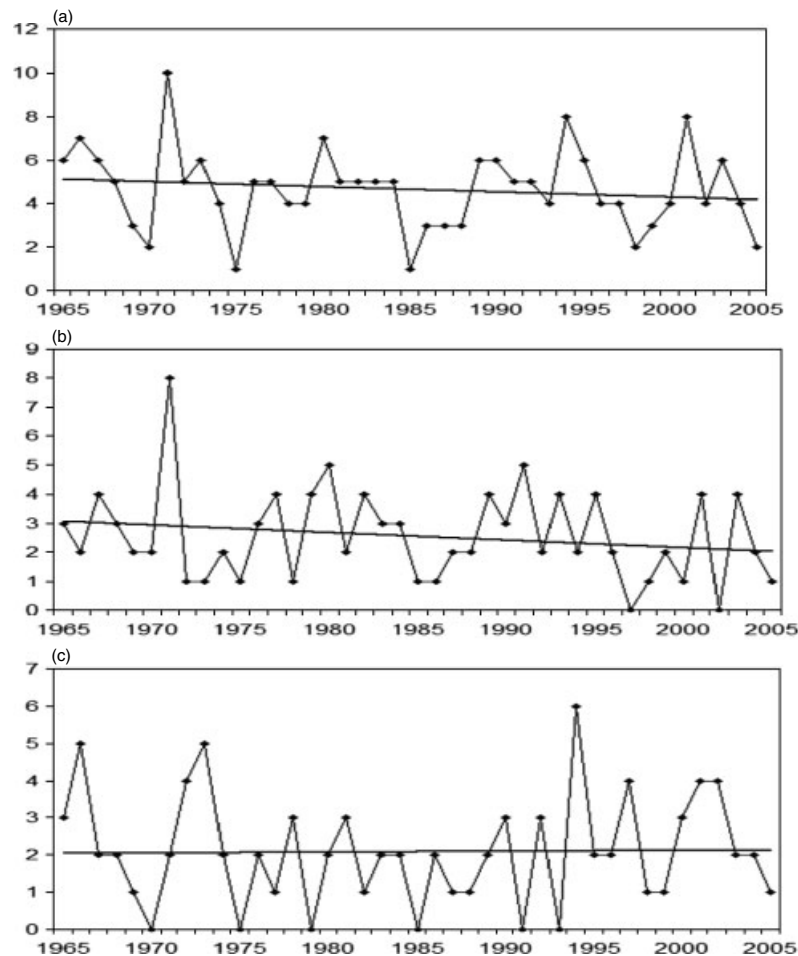
Figure 2. (a) N_T, (b) N_E, and (c) N_F during the early season. The solid straight line indicates the trend.

can be found for the PDO, with N_T, N_E, and N_F being less during PDO+ (Table II). However, the differences between PDO+ and PDO− in all three categories in the late season are not as statistically significant as those for ENSO, reaching only 85% for ENT and 90% for FORM. Nonetheless, it is obvious that the effects of the ENSO and the PDO on TCs are more prominent in the late season, which is reasonable as this is the time when these two phenomena peak.

A comparison of the number of years with above- or below-normal TC activity shows that TC behaviour during EN and LN are mostly opposite, with EN favouring below-normal N_T and N_E (Table III). However, the situation for FORM is similar in EN and LN. This suggests that the effect of ENSO is less on TCs formed in the

Table I. Average N_T, N_E, and N_F in different seasons during EN and LN.

	EN (12 events)			LN (10 events)		
	Whole	Early	Late	Whole	Early	Late
N_T	8.5	4.8	3.7	11.2	4.3	6.9
N_E	4.5	2.3	2.2	6.6	2.3	4.3
N_F	4.0	2.5	1.5	4.6	2.0	2.6

Table II. Same as Table I, except for PDO+ and PDO−.

	PDO Positive (16 years)			PDO Negative (13 years)		
	Whole	Early	Late	Whole	Early	Late
N_T	8.7	4.4	4.3	11.2	5.2	6.0
N_E	5.4	2.6	2.8	6.4	2.6	3.8
N_F	3.3	1.8	1.5	4.7	2.5	2.2

Table III. TC occurrences in different seasons during EN and LN. x/y represents x years in which TC number is above normal/y years in which TC number is below normal.

	EN (12 events)			LN (10 events)		
	Whole	Early	Late	Whole	Early	Late
N_T	1/5	2/1	0/5	5/1	3/3	7/0
N_E	3/6	3/4	2/8	4/2	2/3	5/1
N_F	5/4	5/3	2/1	4/1	2/3	5/1

SCS. Similarly, below-normal TC activities are favoured during PDO+, while the opposite is true during PDO− (Table IV). Again, the effect in the late season is especially prominent, as discussed above.
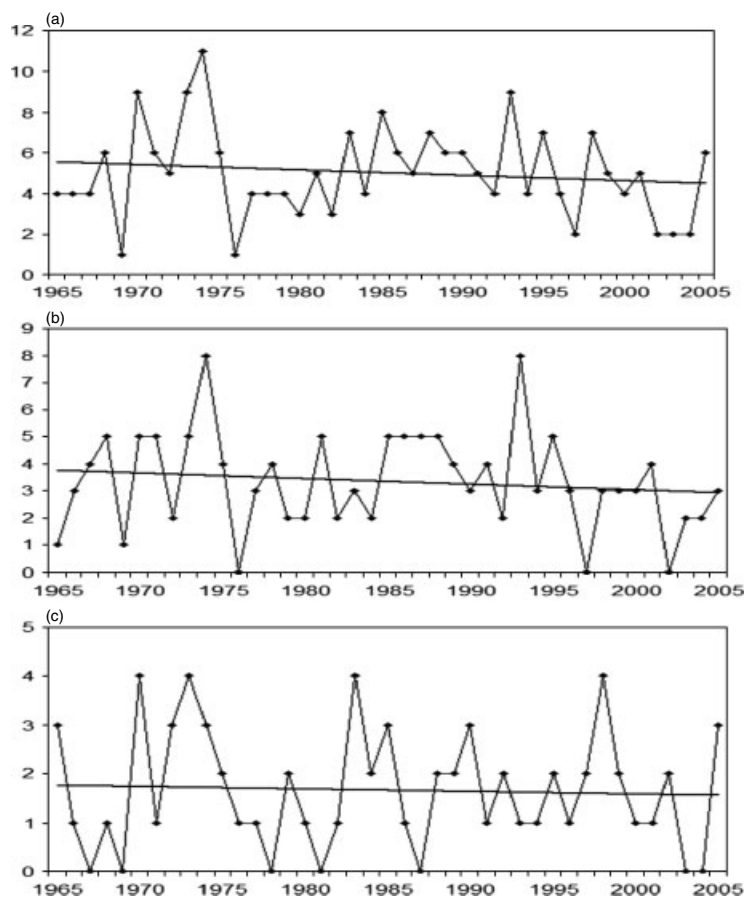
Figure 3. (a) N_T, (b) N_E, and (c) N_F during the late season. The solid straight line indicates the trend.

Table IV. Same as Table III, except for PDO+ and PDO−.

	PDO Positive (16 years)			PDO Negative (13 years)		
	Whole	Early	Late	Whole	Early	Late
N_T	4/7	3/4	3/6	7/1	6/5	5/0
N_E	4/5	6/4	5/10	4/2	2/3	5/1
N_F	4/6	3/6	2/3	5/1	7/5	4/0

4. Factors affecting late-season TC behaviour during ENSO and PDO

As the difference in both N_F and N_E between different phases of the ENSO and the PDO is not statistically significant during the early season, this study only focuses on the situation during the late season. To investigate the reason for the observed differences in TC behaviour, seven factors that affect TC behaviour, namely, 500-hPa zonal wind (500U), 200-hPa divergence (DIV), 500-hPa geopotential height (500H), 850-hPa geopotential height (850H), MSE, 200-850-hPa shear (SHR), and 850-hPa vorticity (VOR), are chosen on the basis of the various studies discussed in Section 1. A correlation-based empirical orthogonal function (EOF) analysis is then employed using the standardized anomalies of the above factors. Two advantages of EOF analysis are that it can identify the key "patterns", and the significance

of the patterns themselves is ranked by the percentage of the variance of the data they explain (Leoncini *et al.*, 2008). In this study, the first three EOFs that explain the most variance for each of the factors are extracted respectively. The total of 21-factor EOFs are then used in a stepwise regression analysis to determine which eight contribute the most to explaining the observed TC behaviour under the different scenarios (EN, LN, PDO+, PDO−). Limiting the number of factors chosen to eight is to avoid having a large number of factors chosen, so as to minimize the risk that some of the chosen factors are not independent from each other (Paeth *et al.*, 2006). With the eight-factor EOFs determined, their behaviour in different phases of the ENSO and the PDO is then examined to investigate their effects on TCs. The domain used in the calculation is between 0° to 45°N, and 100°E to 160°E, and the method of North *et al.* (1982) is used to estimate the sampling errors in EOFs. In the following, the last number in the abbreviations of the factors indicates the EOF, 1 for the first EOF, 2 for the second, etc.

4.1. FORM in the late season

The linear regression equation is given by

$$\text{FORM}_l = 0.019 + 0.315 \times 500U_1 - 0.387 \times 500U_2$$
$$- 0.047 \times \text{DIV}_1 - 0.188 \times \text{DIV}_2 - 0.287$$
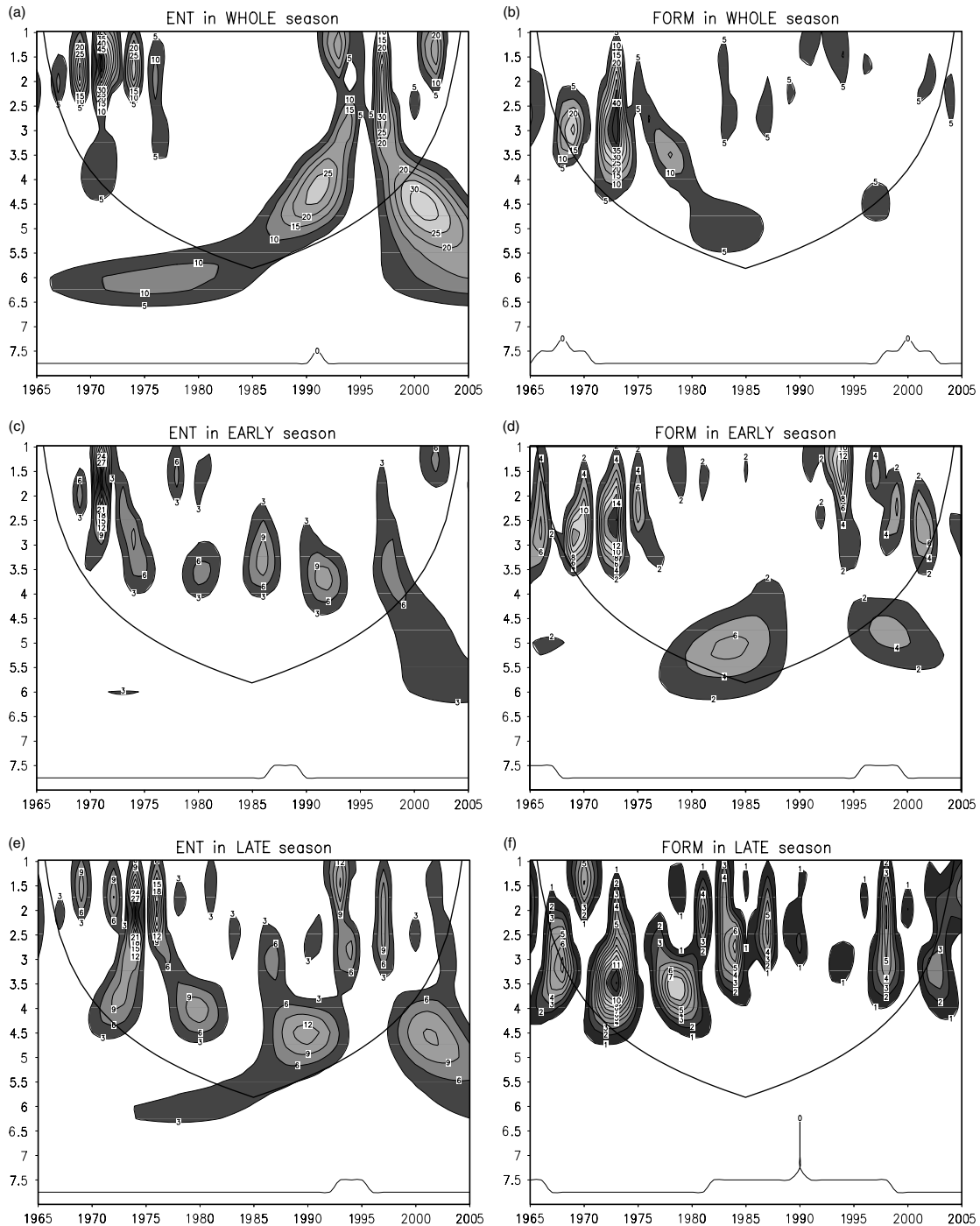
Figure 4. Local wavelet power spectrum of N_E in the (a) whole (c) early and (e) late seasons and of N_F in the (b) whole (d) early and (f) late seasons. Thick solid curve indicates the cone of influence. Value x on y-axis denotes 2 to the power x.

$$\times DIV_3 + 0.193 \times MSE_1 + 0.366$$

$$\times MSE_2 - 0.130 \times SHR_3 \qquad (1)$$

The factor EOFs affecting FORM in the late season are 500U1, 500U2, DIV1, DIV2, DIV3, MSE1, MSE2, and SHR3. This regression equation gives a multiple correlation coefficient of 0.955, which is 95% significant.

4.1.1. ENSO

In general, the flow patterns in EN and LN are quite similar when FORM is considered (Figure 5). Apart from 500U1 and MSE1, both of which indicate that the situation in EN (Figure 5(a) and (f)) is not as favourable to TC genesis as that in LN (Figure 6(a) and (f)), others seem to point out that the major difference between TC behaviour in EN and LN is the location of formation, with less indication on the difference in number. For example, DIV2 (Figures 5(d) and 6(d)), DIV3 (Figures 5(e) and 6(e)), and MSE2 (Figures 5(g) and 6(g)) all indicate favourable situation for TC formation inside the SCS during both phases of ENSO. However, the pattern of DIV3 seems to point out that more TCs form in the
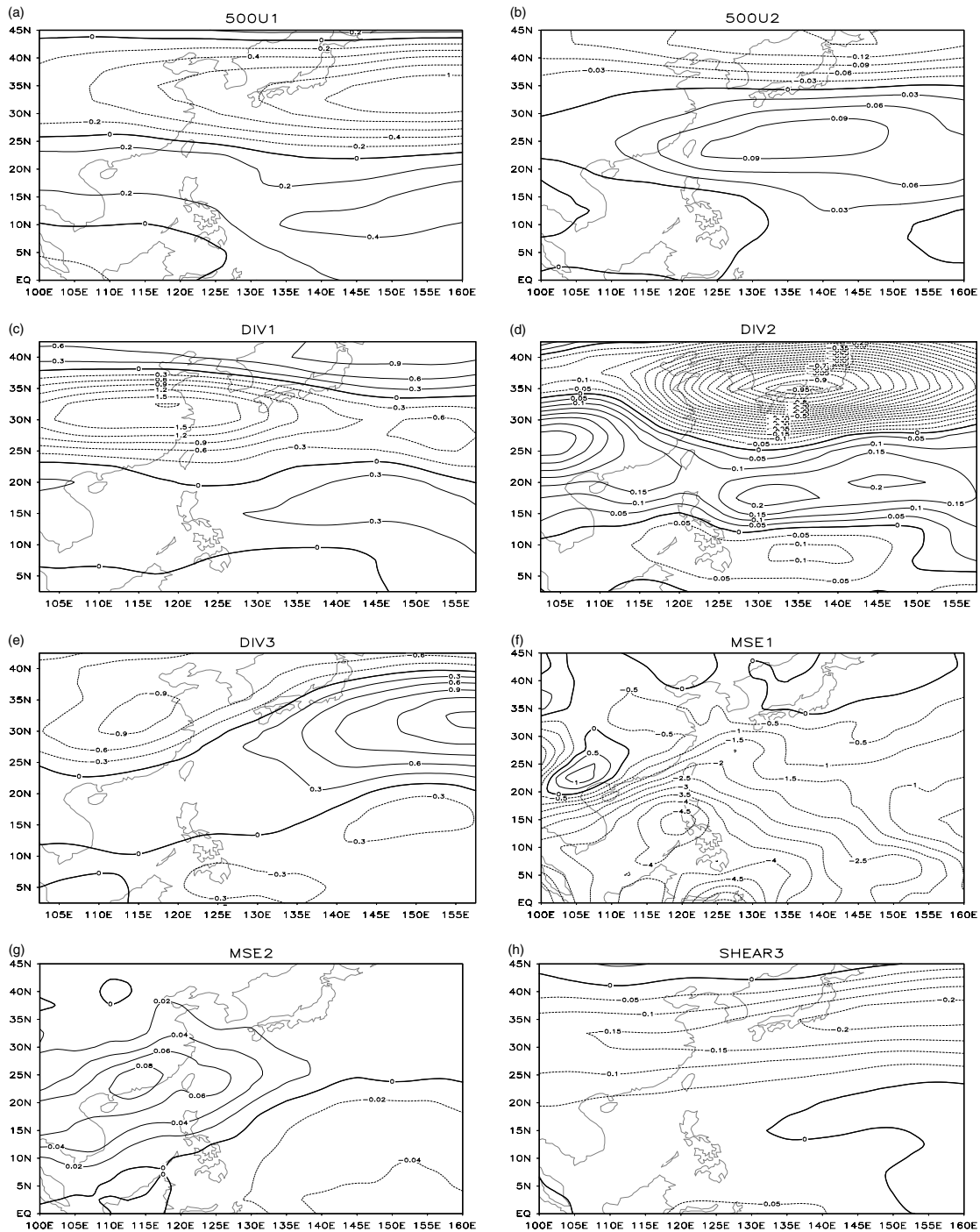
Figure 5. Flow patterns of factor EOFs affecting N_F in the late season during EN. Solid lines indicate positive anomalies, while dotted ones indicate otherwise. (a) 500U1 (Unit: m s^{-1}), (b) 500U2 (Unit: m s^{-1}), (c) DIV1 (Unit: $\times 10^{-6}$ s^{-1}), (d) DIV2 (Unit: $\times 10^{-6}$ s^{-1}), (e) DIV3 (Unit: $\times 10^{-6}$ s^{-1}), (f) MSE1 (Unit: $\times 10^{6}$ W m^{-2}), (g) MSE2 (Unit: $\times 10^{6}$ W m^{-2}), and (h) SHR3 (Unit: m s^{-1}).

northern part of the SCS during EN and more in the south during LN. This is supported by the 500-hPa flow pattern. In the northern SCS, although the pattern of 500U2 suggests an anticyclonic anomaly during both EN (Figure 5(b)) and LN (Figure 6(b)), indicating less-deep convection in the area, the magnitude of this factor EOF is quite small. On the other hand, the pattern of 500U1 in southern SCS reveals a cyclonic anomaly centred over 10°N during LN, whereas the opposite is true during EN. Thus, in the north, the larger DIV2 means more FORM

in this part of the SCS during EN. In the south, the cyclonic flow at 500 hPa is advantageous to the genesis of TCs, and infers more FORM during LN. The situation is opposite during EN, when an anticyclonic flow is found at 500 hPa, inhibiting the formation of TCs and inferring less FORM. Considering the effects of DIV2, DIV3, 500U1, and 500U2, it can be concluded that TCs in EN would preferably form in the northern SCS, while during LN, more TCs are formed in the southern SCS. This is in fact the case, with the average formation latitude
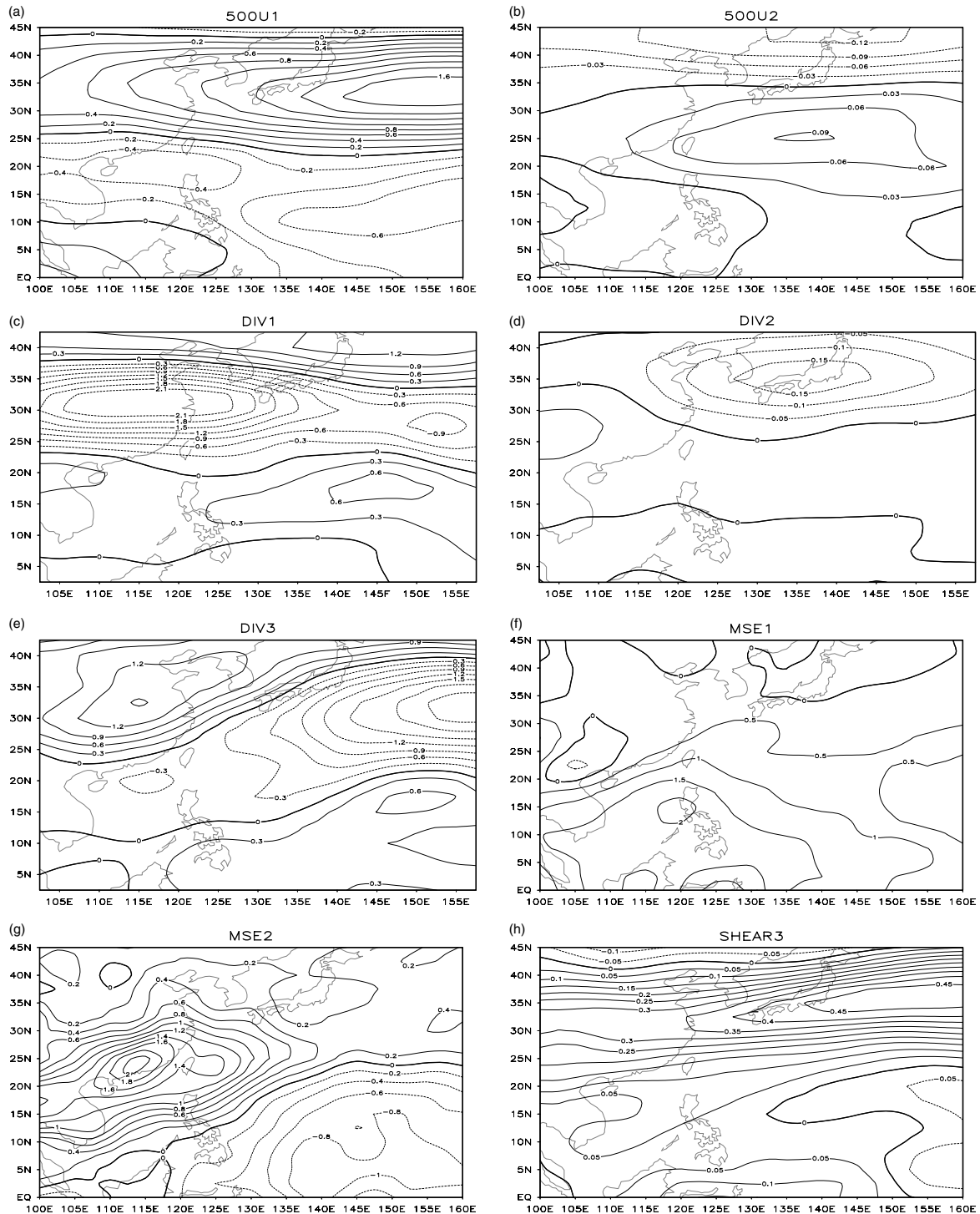
Figure 6. Same as Figure 5, except for LN.

of TCs during EN being 14.8 °N and 12.6 °N during LN, the difference between the two being statistically significant at the 95% confidence level. This north–south discrepancy is not seen in the WNP in the late season, and is opposite to the situation in the early season, where TCs in LN are found to form preferably to the north, while those in EN to the south (Chen *et al.*, 1998).

Various studies have pointed out the relationship between the location of TC formation and the monsoon trough in the WNP (e.g. Lander, 1994; Chen *et al.*, 1998).

Analyses of the 850-hPa flow pattern in the late season (not shown) reveals that the monsoon trough is nearly non-existent inside the SCS during EN, whereas it is located along around 8°N during LN. Outside of the SCS, in the WNP, the eastern tail of the monsoon trough extends along about the same latitude during both phases of the ENSO. Thus, it seems that the absence of the monsoon trough inside the SCS is able to explain the lack of FORM during EN, and that the monsoon trough lies along the same latitude in the WNP during both EN and
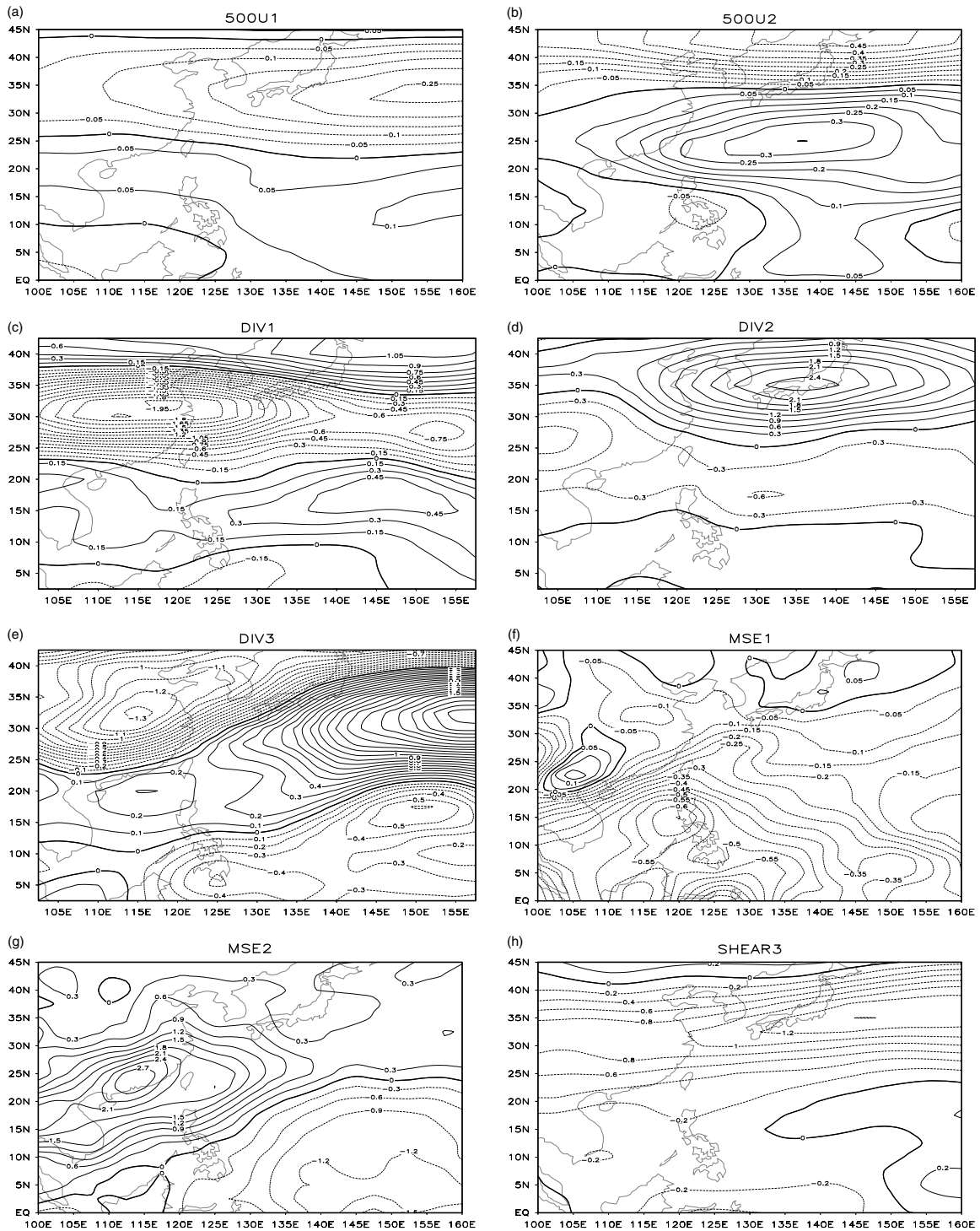
Figure 7. Same as Figure 5, except for PDO+.

LN can account for the lack of north–south discrepancy in TC number in the WNP.

4.1.2. PDO

Although observations suggest that more TCs are formed inside the SCS during PDO−, the factor EOFs seem to give inconclusive results. This could be the reason for the difference between FORM during PDO+ and PDO− being only statistically significant at 90%. Focusing first on the patterns at 500 hPa, during PDO−, both

500U1 (Figure 8(a)) and 500U2 (Figure 8(b)) indicate the presence of strong anticyclonic anomalies associated with the strong zonal wind anomalies in both the northern and southern parts of the SCS. The situation is opposite during PDO+ (Figure 7(a) and (b)). However, because the flow at 500 hPa is more indicative of the movement of tropical cyclones than formation, these anomalies might not have a huge impact on N_F. Of the remaining six-factor EOFs, DIV1 and DIV3 both show similar patterns during the two phases of PDO. However, it is obvious that
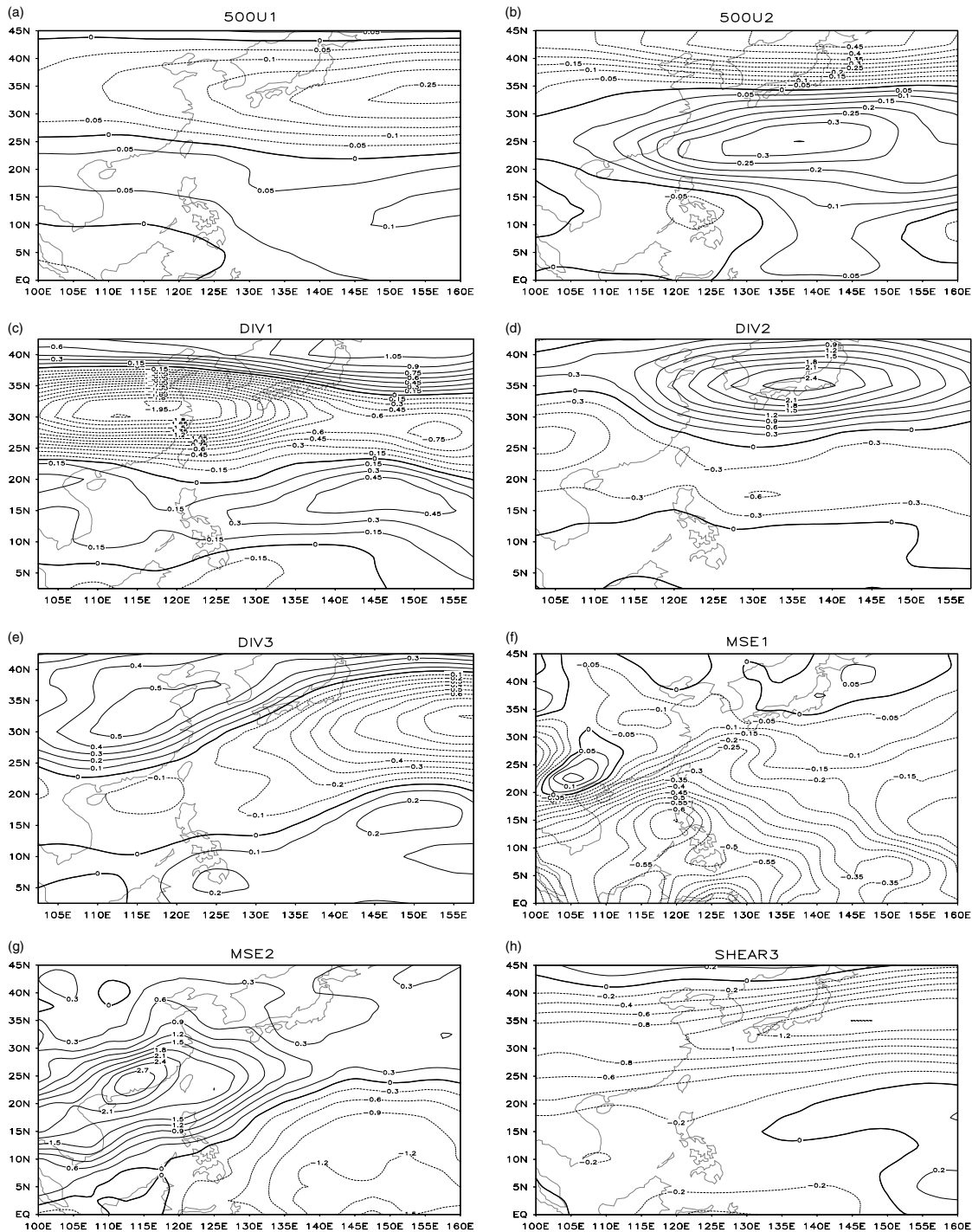
Figure 8. Same as Figure 5, except for PDO−.

the positive anomaly in DIV1 is stronger during PDO− (Figure 8(c)) than during PDO+ (Figure 7(c)), indicating a more favourable condition for TC formation in SCS during this phase of PDO. Although the pattern of DIV3 seems to indicate a more favourable environment in the SCS for FORM during PDO+ (Figure 7(e)), as does that of MSE1 (Figure 7(f)), their effects might not be able to overcome those by the other three factor EOFs, namely, DIV2, MSE2, and SHR3. Of these, the patterns of MSE2 and SHR3 clearly indicate that the situation in the SCS is more conductive to the genesis of TCs during PDO−,

as seen by the strongly positive MSE2 (Figure 8(g)) and negative SHR3 (Figure 8(h)) anomalies.

As for DIV2, its pattern seems to suggest that TC formation is favoured in the southern part and inhibited in the northern part of SCS during PDO−, and vice versa. However, it can be seen that there is no clear north–south difference in the location of TC formation, unlike the ENSO classification, which might be explained by the fact that the monsoon troughs during both PDO+ and PDO− run northeastwards from roughly 4°N to 9°N inside the SCS.
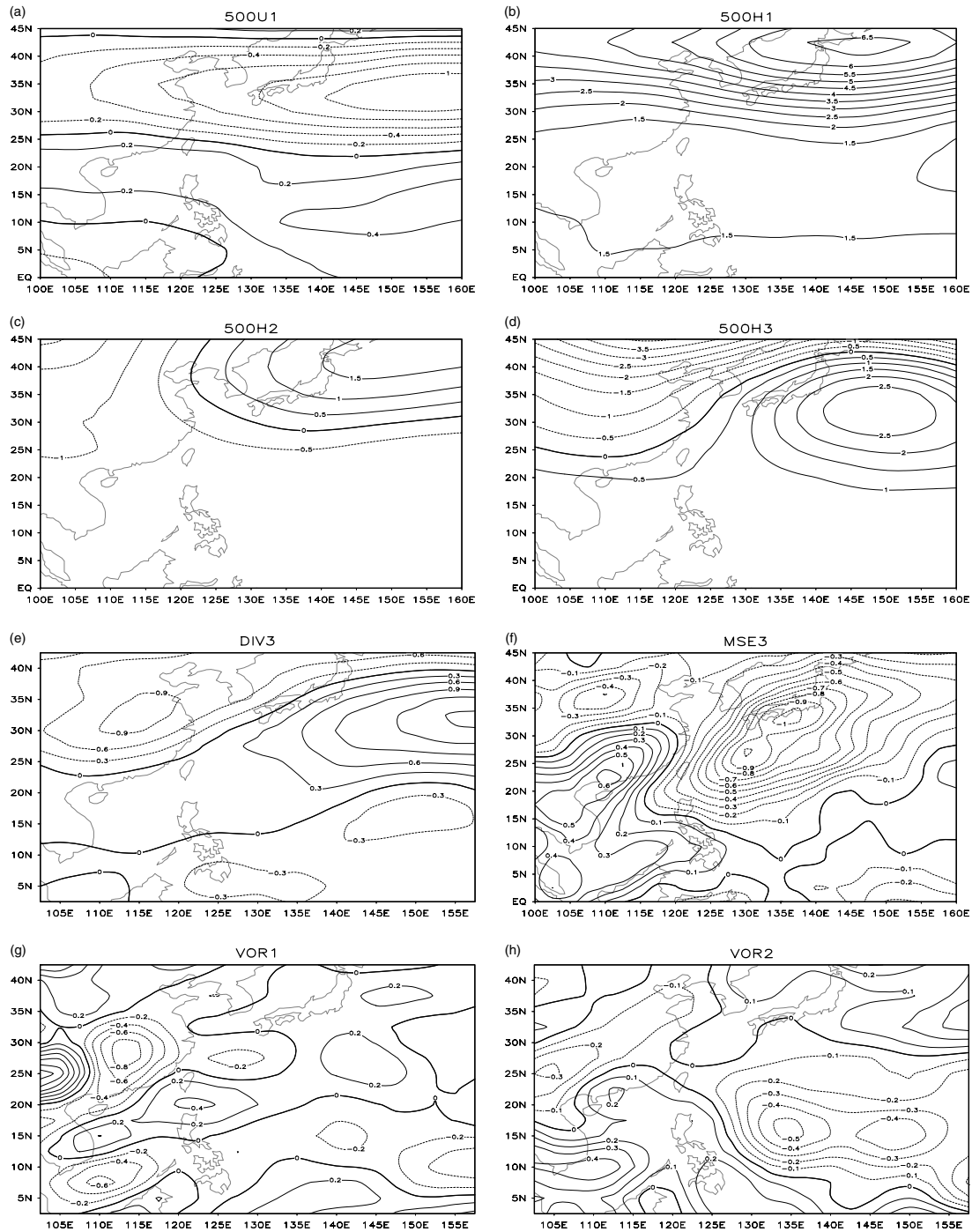
Figure 9. Flow patterns of factor EOFs affecting N_E in the late season during EN. Solid lines indicate positive anomalies, while dotted ones indicate otherwise. (a) 500U1 (Unit: m s^{-1}), (b) 500H1 (Unit: gpm), (c) 500H2 (Unit: gpm), (d) 500H3 (Unit: gpm), (e) DIV3 (Unit: $\times 10^{-6}$ s^{-1}), (f) MSE3 (Unit: $\times 10^6$ W m^{-2}), (g) VOR1 (Unit: $\times 10^{-6}$ s^{-1}), and (h) VOR2 (Unit: $\times 10^{-6}$ s^{-1}).

4.2. ENT in the late season

The linear regression equation is given by

$$
\begin{aligned}
\mathrm{ENT}_l = {} & -0.098 + 1.422 \times 500\mathrm{U}_1 + 0.179 \\
& \times \mathrm{DIV}_3 + 1.333 \times \mathrm{HGT}_1 - 0.539 \times \mathrm{HGT}_2 \\
& -0.448 \times \mathrm{HG\,T}_3 + 0.349 \times \mathrm{MSE}_3 - 0.575 \\
& \times \mathrm{VOR}_1 + 0.301 \times \mathrm{VOR}_2 \qquad (2)
\end{aligned}
$$

This regression equation gives a multiple correlation coefficient of 0.956, which is significant at the 95% confidence level, and suggests that the eight-factor EOFs affecting ENT in the late season are 500U1, 500H1, 500H2, and 500H3 (the steering factors), and DIV3, MSE3, VOR1, and VOR2 (the genesis factors).

4.2.1. ENSO

Figures 9 and 10 show the behaviour of the factor EOFs affecting ENT during EN and LN, respectively. Recall
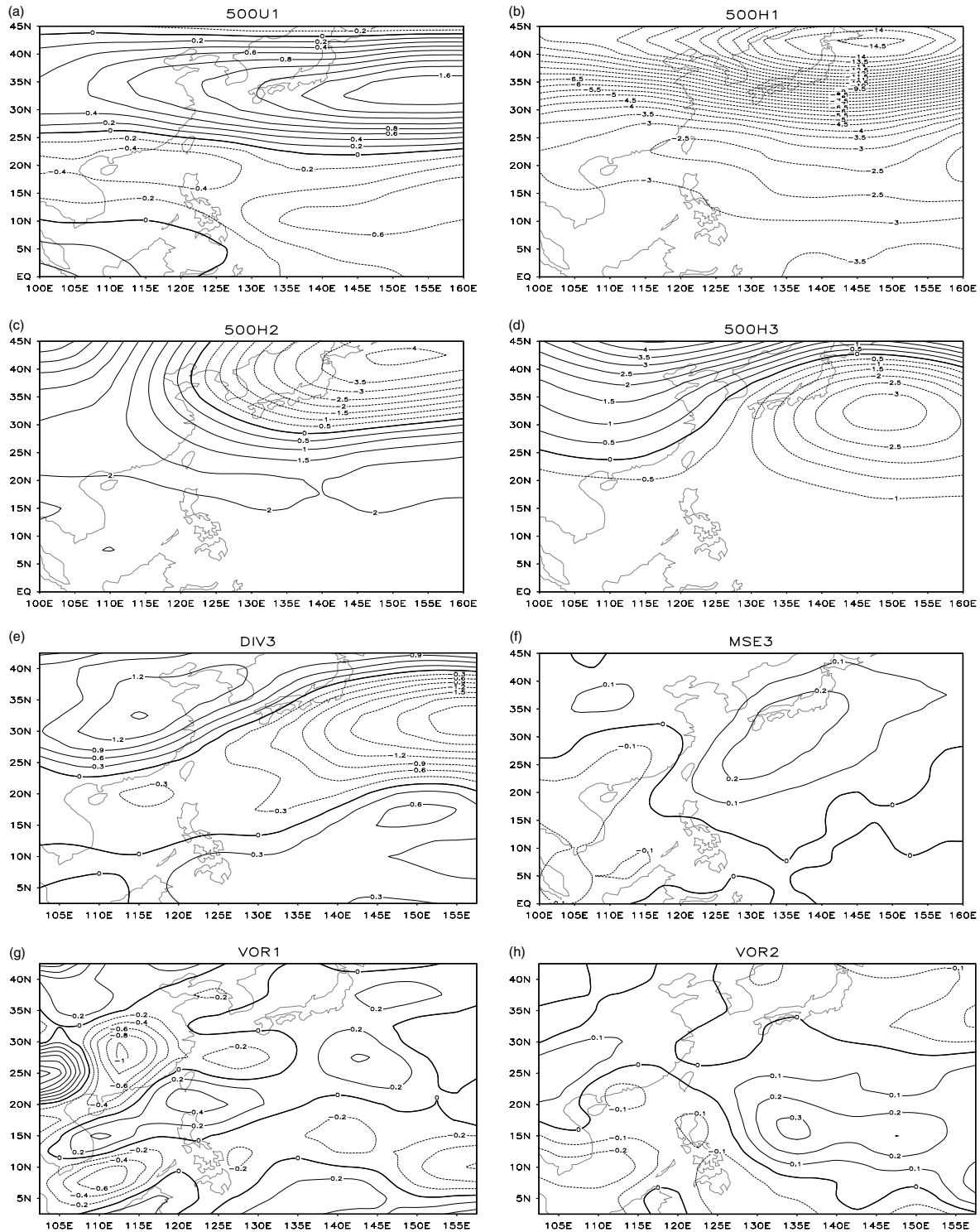
Figure 10. Same as Figure 9, except for LN.

that ENT in the late season is less during EN and more during LN. Indeed, the genesis factors indicate that in general, fewer TCs are formed in the EOF analysis domain over the WNP during EN. This could be due to the fact that TCs tend to form more towards the east and the south during EN so that the EOF analysis indicates below-normal formation near the Philippines. At the same time, all the steering factors, except 500H1 (Figure 9(b)), suggest that the situation during EN does not favour TCs

being steered into the SCS. Specifically, the patterns of 500H2 (Figure 9(c)) and 500H3 (Figure 9(d)) suggest a southeasterly to southerly flow around 130 °E. Considering the formation location of TCs during EN, it is likely that those TCs are caught in this flow, causing them to recurve. On the other hand, although there is no conclusive evidence that more TCs are steered into the SCS during LN, the genesis factors indicate that more TCs are formed in the WNP, which may explain the higher
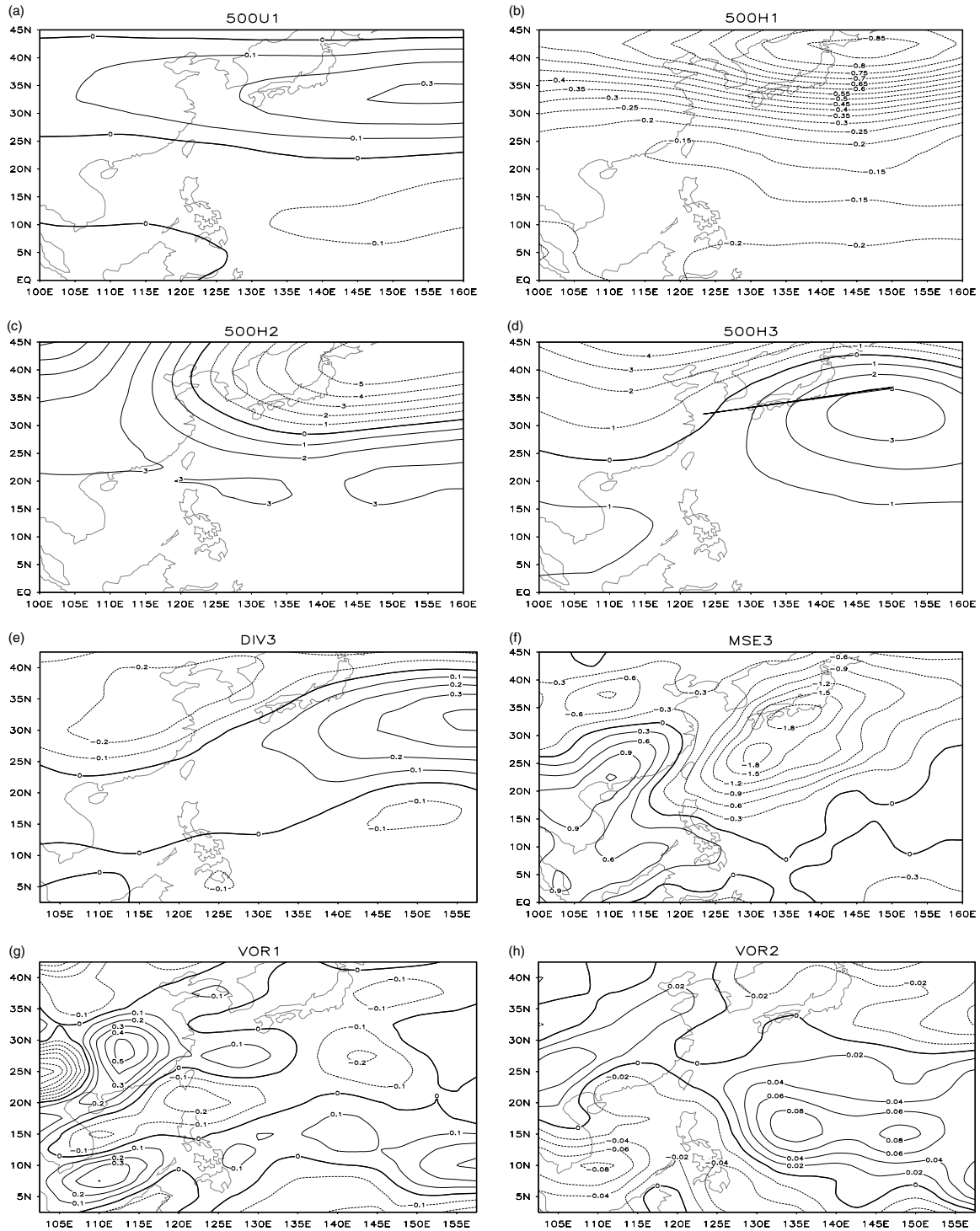
Figure 11. Same as Figure 9, except for PDO+.

N_E during this phase of ENSO. It can be seen that all the EOFs of 500-hPa geopotential height exhibit above-normal anomaly during EN and vice versa during LN. Chan (1985) indicated that during EN, an anomalous Walker circulation would be formed, such that sinking motion could be found in the western WNP. The anomalous high pressure is the result of this sinking motion, and this subsidence would inhibit TC activities. Various literature also agrees that the anomalous Walker circulation would affect TC genesis location and thus activities

(e.g. Chen *et al.*, 1998; Wang and Chan, 2002). Thus, this at least partly explains the below-normal N_E observed during EN.

4.2.2. PDO

Similar to the situation for FORM, the factor EOFs provide inconclusive evidence for explaining the observed difference between N_E during PDO+ and PDO−, and this may account for this value to be significant only at
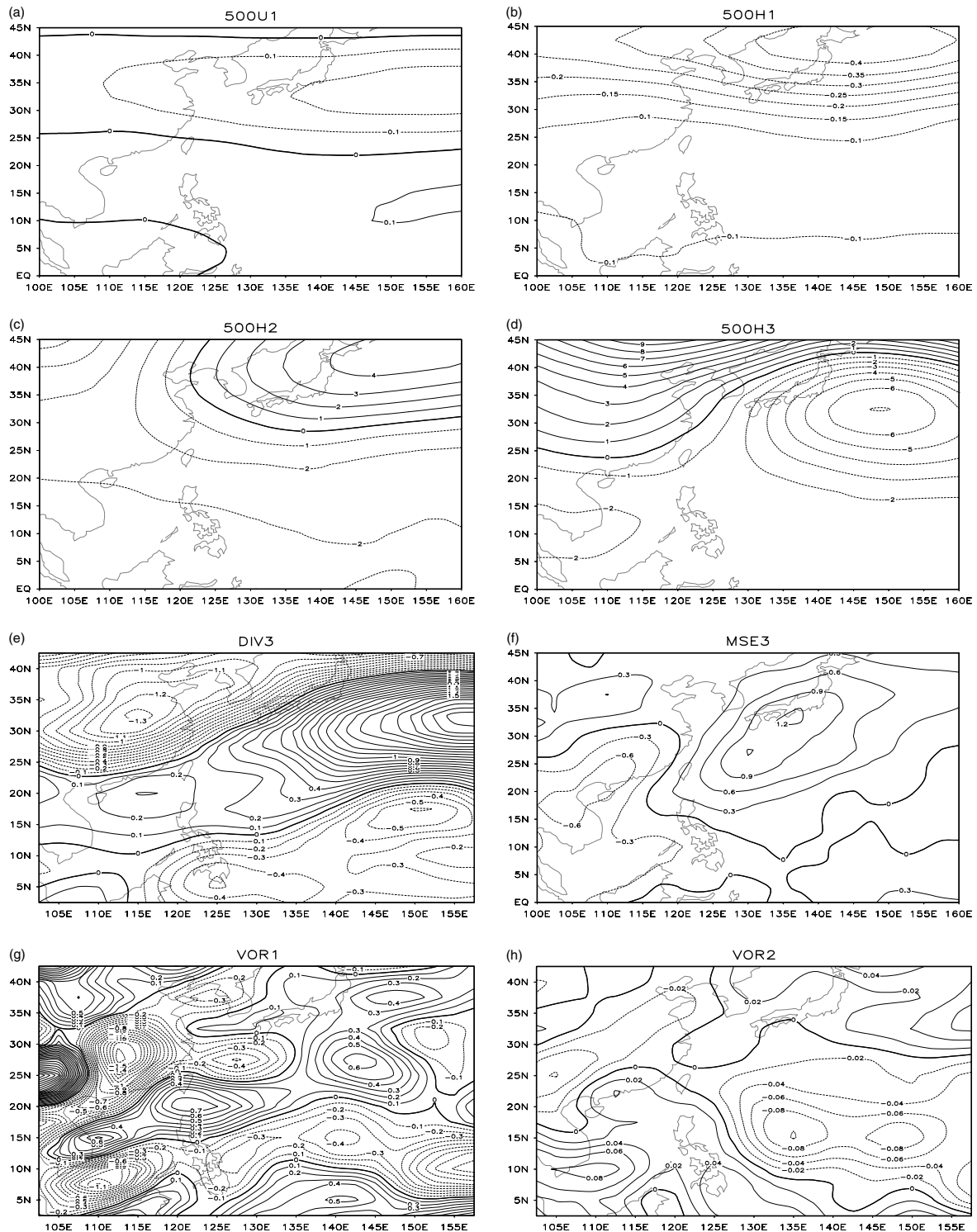
Figure 12. Same as Figure 9, except for PDO−.

the 85% confidence level. Focusing first on TC genesis, the DIV3 patterns (Figures 11(e) and 12(e)) are similar, indicating favourable conditions for the formation of TCs in the WNP, during both phases of the PDO, whereas the patterns of MSE3 (Figure 12(f)), VOR1 (Figure 12(g)), and VOR2 (Figure 12(h)) point to more TCs being formed in the WNP east of the Philippines and less in the seas further to the east during PDO−, and vice versa.

Switching to the movement factor EOFs, the 500U1 pattern shows negative, or easterly, anomalies over the SCS and WNP south of 23 °N during PDO+ (Figure 11(a)), which is a favourable condition for TCs to be steered into the SCS. However, the pattern of 500H2 (Figure 11(c)) shows an anomalous low to the east of Japan, which causes an anomalous cyclonic flow over the WNP. Along with this is an anomalous high centred along 18 °N, with a break between 135 °E and 145 °E.

This pattern would steer TCs formed in the low latitudes of the WNP to the northwest through the break, and then into the westerly flow caused by the anomalous low to the east of Japan. The result is the recurvature of TCs during PDO+. On the contrary, during PDO−, the anomalous high becomes an anomalous low, leading to anomalous easterlies over the WNP, which help in steering TCs into the SCS (Figure 12(c)). The pattern of 500H3 brings a similar effect, but this time, an anomalous high is centred over the WNP east of Japan during PDO+, causing an anticyclonic flow to prevail over the area west of $145\,°E$ and north of $15\,°N$. TCs formed in the lower latitudes passing through the area would get caught in the southeasterlies due to the anticyclone and be steered northwestward, then northward, causing them to recurve before reaching the SCS (Figure 11(d)). During PDO−, an anomalous high is situated over Siberia, which brings easterlies to the seas south of Taiwan (Figure 12(d)). Recall that during this phase of the PDO, cyclogenesis is favoured in the WNP to the east of the Philippines. Thus, it is quite possible for those TCs to be caught in these anomalous easterlies and be steered into the SCS.

So it seems that the major effect of the PDO on ENT is on their tracks. Even though cyclogenesis is favoured over much of the WNP, TCs during PDO+ are more prone to recurving, and thus contributing to a below-normal N_E. During PDO−, although the favourable area for TC formation is confined to the WNP east of the Philippines, the steering flow is such that the TCs formed in that area could easily be steered into the SCS. It is noteworthy that, similar to the situation during EN, the flow at 500 hPa seems to favour recurvature of TCs during PDO+. This could be the result of the forcing of PDO by ENSO, as described by Newman *et al.* (2003), where a positive phase of PDO is the result of an EN during the previous few seasons, and similarly, a negative phase of PDO is due to an LN.

5. Summary and discussion

This study has shown that, similar to their counterparts in the WNP, SCS TCs also show interannual and interdecadal variations in number. The number of TCs entering the SCS (N_E) has shown a decreasing trend over the study period in both the early (May to August) and late (September to December) seasons, while that formed in the SCS (N_F) has not changed significantly over the years.

Wavelet analyses have lent support to the hypothesis that TC activities in the SCS are modulated by ENSO. Specifically, N_E in the whole and late seasons shares the same periodicity with the ENSO before 1976, as is N_F in the early season. N_E in the early and late seasons, as well as N_F in the late season, also show longer periodicities, which could be related to the PDO. As for TC activity, N_E and N_F during EN and PDO+ tend to be below normal, while above-normal TC activity is found during LN and PDO−.

The cause for all these differences and trends in N_E and N_F can be traced back to the behaviour of their respective factor EOFs, most of which are affected by the ENSO and the PDO. Analyses of factors affecting ENT indicate that TCs formed in the WNP are subsequently steered into the SCS by the 500-hPa flow. The flow patterns during both LN and PDO− are generally easterlies, and thus are favourable for TCs to be steered into the SCS. On the contrary, during EN and PDO+, the steering flow tends to cause TCs to recurve such that they cannot reach the SCS.

The conditions within the SCS are crucial in determining the behaviour of FORM, as results indicate that TCs formed inside the basin are generally not due to convection from outside being steered into the SCS. In general, TC formation is inhibited during EN but favoured during LN. An interesting point to note is the north–south discrepancy in TCs formed between EN and LN, which is found to be the result of the difference in the location and strength of the monsoon trough during these two phases of ENSO. However, this disparity is not seen in the PDO cases, apparently due to the location of monsoon trough being virtually constant between the two PDO phases. The difference in N_F between PDO+ and PDO− is also not as obvious as that in the ENSO cases.

Thus, it is apparent that, similar to the situation in the WNP, the interannual and interdecadal variations in TC activity inside the SCS are largely related to ENSO and PDO, which causes variations in the factors affecting TC behaviour. With the factors affecting N_E and N_F in both seasons known and the relationship between these factors and ENSO and PDO established, predictions of TC activity in the SCS can be carried out. This could be accomplished by predicting the behaviour of the factors using their relationship with ENSO and PDO. Since the skill in the prediction of these large-scale atmospheric phenomena, especially that of ENSO, is already relatively well developed, a good prediction of TC activities in the SCS would certainly be possible and worth attempting, and will be the next step in this study.

Appendix

A1. ENSO events

Table AI summarizes the 12 EN events and 10 LN events, as defined in Section 2.2, from 1965 to 2005.

Table AI. Start and end dates, the duration, and the ENSO index for EN and LN events since 1965. Events linked by a square bracket (]) denotes "coupled events" as defined in the text. Asterisk indicates the 1993 event not included in this study.

EN (12 events)				LN (10 events)			
Start	End	Duration	Index	Start	End	Duration	Index
1965.6	1966.4	11	1.2	1967.9	1968.5	9	−0.7
1968.11	1970.1	15	1	1970.5	1972.1	21	−1.4
1972.5	1973.3	11	1.8	1973.5	1974.7	15	⌐−1.8
1976.9	1977.2	18	⌐0.6	1974.9	1976.5	21	−0.6
1977.9	1978.2	6	0.7	1983.9	1984.2	6	⌐−0.5
1982.5	1983.6	14	2.3	1984.10	1985.9	12	−1
1986.8	1988.2	19	1.3	1988.5	1989.6	14	−1.7
1991.5	1992.6	14	1.8	1995.9	1996.3	7	−0.8
1993.2	1993.9	8*	–	1998.7	2000.7	25	⌐−1.6
1994.3	1995.4	14	1.2	2000.9	2001.3	7	−0.7
1997.4	1998.5	14	2.4	–	–	–	–
2002.4	2003.3	12	1.1	–	–	–	–
2004.6	2005.2	9	0.6	–	–	–	–

Table AII. Positive and negative PDO events since 1965.

Positive (16 events)	Negative (13 events)
1969, 1976, 1979, 1980, 1982, 1983, 1984, 1985, 1986, 1987, 1992, 1993, 1995, 1997, 2002, 2003.	1965, 1966, 1968, 1970, 1971, 1973, 1975, 1988, 1990, 1994, 1998, 1999, 2001.

Square bracket (]) denotes "coupled events", in which the SST anomalies remained of one sign, even though the value fell below the ±0.4 °C threshold (Trenberth, 1997). Furthermore, some studies (e.g. Trenberth, 1997) considered the 1993 event, indicated by an asterisk (*), as a very weak event or a continuation of the 1991–1992 event. Thus, it is not included in this study.

A2. PDO events

Positive and negative PDO events, as defined in Section 2.2 of the text, are listed in Table AII. In total, there are 16 PDO+ and 13 PDO− events between 1965 and 2005.

References

Briegel LM, Frank WM. 1997. Large-scale influences on tropical cyclogenesis in the Western North Pacific. *Monthly Weather Review* **125**: 1397–1413.

Chan JC-L. 1985. Tropical cyclone activity in the northwest Pacific in relation to the El Niño/Southern Oscillation phenomenon. *Monthly Weather Review* **113**: 599–606.

Chan JC-L. 1995. Tropical cyclone activity in the western North Pacific in relation to the stratospheric quasi-biennial oscillation. *Monthly Weather Review* **123**: 2567–2571.

Chan JC-L. 2000. Tropical cyclone activity over the Western North Pacific associated with El Niño and La Niña events. *Journal of Climate* **13**: 2960–2972.

Chan JC-L. 2005. Interannual and interdecadal variations of tropical cyclone activity over the Western North Pacific. *Meteorology and Atmospheric Physics* **89**: 143–152.

Chan JC-L, Gray WM. 1982. Tropical cyclone movement and surrounding flow relationships. *Monthly Weather Review* **110**: 1354–1374.

Chan JC-L, Liu KS. 2004. Global warming and Western North Pacific typhoon activity from an observational perspective. *Journal of Climate* **17**: 4590–4602.

Chan JC-L, Shi JE. 1996. Long-term trends and interannual variability in tropical cyclone activity over the Western North Pacific. *Geophysical Research Letters* **23**: 2765–2767.

Chan JC-L, Williams RT. 1987. Numerical studies of the beta effect in tropical cyclone motion. Part 1: Zero mean flow. *Journal of the Atmospheric Sciences* **44**: 1257–1265.

Chan JC-L, Williams RT. 1994. Numerical studies of the beta effect in tropical cyclone motion. Part 2: Zonal mean flow effects. *Journal of the Atmospheric Sciences* **51**: 1065–1076.

Chen T-C, Weng S-P, Yamazaki N, Kiehne S. 1998. Interannual variation in the tropical cyclone formation over the Western North Pacific. *Monthly Weather Review* **126**: 1080–1090.

Chia HH, Ropelewski CF. 2002. The interannual variability in the genesis location of tropical cyclones in the Northwest Pacific. *Journal of Climate* **15**: 2934–2944.

Emanuel A. 1993. The physics of tropical cyclone genesis over Eastern Pacific. *Tropical Cyclone Disasters*, Lighthill J, Zhemin Z, Holland GJ, Emanuel K (eds). Peking University Press: Beijing, China; 136–142.

George JE, Gray WM. 1976. Tropical cyclone motion and surrounding parameter relationships. *Journal of Applied Meteorology* **15**: 1252–1264.

Gray WM. 1968. Global view of the origin of tropical disturbances and storms. *Monthly Weather Review* **96**: 669–700.

Gray WM. 1979. Hurricanes: their formation, structure and likely role in the tropical circulation. In *Meteorology Over Tropical Oceans*, Shaw DB (ed.). Royal Meteorological Society: James Glaisher House, Grenville Place, Bracknell, Berkshire, RG12 1BX; 155–218.

Hare SR, Mantua NJ. 2000. Empirical evidence for North Pacific regime shifts in 1977 and 1989. *Progress in Oceanography* **47**: 103–145.

Ho C-H, Baik J-J, Kim J-H, Gong D-Y, Sui C-H. 2004. Interdecadal changes in summertime typhoon tracks. *Journal of Climate* **17**: 1767–1776.

Kalnay E, *et al*. 1996. The NCEP/NCAR 40-year reanalysis project. *Bulletin of the American Meteorological Society* **77**: 437–471.

Lander MA. 1994. An exploratory analysis of the relationship between tropical storm formation in the Western North Pacific and ENSO. *Monthly Weather Review* **122**: 6636–6651.

Lee C-S, Lin Y-L, Cheung KKW. 2006. Tropical cyclone formations in the South China Sea associated with the Mei-yu front. *Monthly Weather Review* **134**: 2670–2687.

Leoncini G, Pielke RA Sr, Gabriel P. 2008. From model-based parameterizations to lookup tables: an EOF approach. *Weather and Forecasting* **23**: 1127–1145.

Leung YK, Wu MC, Chang WL. 2005. Variations of tropical cyclone activity in the South China Sea. Presented in ESCAP/WMO Typhoon Committee Annual Review 2005, November 2006. *Hong Kong Observatory Reprint No.* **675**.

Li C. 1988. Actions of typhoons over the western Pacific (including the South China Sea) and El Niño. *Advances in Atmospheric Sciences* **5**: 107–115.

Lighthill J, Holland G, Gray W, Landsea C, Craig G, Evans J, Kurihara Y, Guard C. 1994. Global climate change and tropical cyclones. *Bulletin of the American Meteorological Society* **75**: 2147–2157.

Liu KS, Chan JC-L. 2003. Climatological characteristics and seasonal forecasting of tropical cyclones making landfall along the South China Coast. *Monthly Weather Review* **131**: 1650–1662.

Liu KS, Chan JCL. 2006. Interdecadal variability of Western North Pacific tropical cyclone activity. *Presented in the 27th Conference on Hurricanes and Tropical Meteorology*. American Meteorological Society: Monterey, CA.

Mantua NJ. 1999. The Pacific Decadal Oscillation and climate forecasting for North America. *Climate Risk Solutions Newsletter, Maryam Golnaraghi (Ed.)* **1**: 10–13.

McBride JL, Zehr RM. 1981. Observational analysis of tropical cyclone formation. Part II: Comparison of non-developing versus developing systems. *Journal of the Atmospheric Sciences* **38**: 1132–1151.

Neumann CJ. 1992. The Joint Typhoon Warning Center (JTWC92) model. *SAIC, Final Report, Contract No. N00014-90-C-6042*, 85.

Newman M, Compo GP, Alexander MA. 2003. ENSO-forced variability of the Pacific Decadal Oscillation. *Journal of Climate* **16**: 3853–3857.

North GR, Bell TL, Cahalan RF, Moeng FJ. 1982. Sampling errors in the estimation of empirical orthogonal functions. *Monthly Weather Review* **110**: 699–706.

Paeth H, Girmes R, Menz G, Hense A. 2006. Improving seasonal forecasting in the low latitudes. *Monthly Weather Review* **134**: 1859–1879.

Ramsay HA, Leslie LM, Lamb PJ, Richman MB, Leplastrier M. 2008. Interannual variability of tropical cyclones in the Australian region: role of large-scale environment. *Journal of Climate* **21**: 1083–1103, DOI: 10.1175/2007JCLI1970.1.

Santer BD, Wigley TML, Boyle JS, Gaffen DJ, Hnilo JJ, Nychka D, Parker DE, Taylor KE. 2000. Statistical significance of trends and trend differences in layer-average atmospheric temperature time series. *Journal of Geophysical Research* **105**: 7337–7356.

Schneider N, Cornuelle BD. 2005. The forcing of the PDO. *Journal of Climate* **18**: 4355–4373.

Song Y, Lau K-M, Kim K-M. 2002. Variations of the East Asian jet stream and Asian–Pacific–American winter climate anomalies. *Journal of Climate* **15**: 306–325.

Stowasser M, Wang Y, Hamilton K. 2007. Tropical cyclone changes in the Western North Pacific in a global warming scenario. *Journal of Climate* **20**: 2378–2396.

Torrence C, Compo GP. 1998. A practical guide to wavelet analysis. *Bulletin of the American Meteorological Society* **79**: 61–78.

Trenberth KE. 1997. The definition of El Niño. *Bulletin of the American Meteorological Society* **78**: 2771–2777.

Wang B, Chan JC-L. 2002. How strong ENSO events affect tropical storm activity over the Western North Pacific. *Journal of Climate* **15**: 1643–1658.

Wang L, Fung CH, Lau KH. 2007a. The upper ocean thermal structure and the genesis locations of tropical cyclones in the South China Sea. *Journal of Ocean University of China* **6**: 125–131.

Wang L, Lau K-H, Fung CH, Gan JP. 2007b. The relative vorticity of ocean surface winds from the QuikSCAT satellite and its effects on the geneses of tropical cyclones in the South China Sea. *Tellus A* **59**: 562–569.

Wu MC, Chang WL, Leung WM. 2004. Impacts of El Niño–Southern Oscillation events on tropical cyclone landfalling activity in the Western North Pacific. *Journal of Climate* **17**: 1419–1428.

Wu R, Kinter JL III, Kirtman BP. 2005. Discrepancy of interdecadal changes in the Asian region among the NCEP–NCAR reanalysis, objective analyses, and observations. *Journal of Climate* **18**: 3048–3067.

Yeh S-W, Kirtman B. 2004. The North Pacific Oscillation–ENSO and internal atmospheric variability. *Geophysical Research Letters* **31**: L13206, DOI:10.1029/2004GL019983.

Yeung KH, Wu MC, Chang WL, Leung YK. 2005. Long-term change in tropical cyclone activity in the Western North Pacific. In *Presented in the Scientific Assembly of International Association of Meteorology and Atmospheric Science (IAMAS) 2005*, Beijing, China, 2-11 August, 2005. *Hong Kong Observatory Reprint No.* **601**.

Yumoto M, Matsuura T. 2001. Interdecadal variability of tropical cyclone activity in the Western North Pacific. *Journal of the Meteorological Society of Japan* **79**: 23–35.